Microchim Acta (2011) 175:283–289
DOI 10.1007/s00604-011-0684-2

ORIGINAL PAPER

Carbon fiber microelectrodes modified with carbon nanotubes as a new support for immobilization of glucose oxidase

Hao Wen · Vijayadurga Nallathambi · Deboleena Chakraborty · Scott Calabrese Barton

Received: 18 May 2011 / Accepted: 11 August 2011 / Published online: 27 August 2011

Abstract Carboxylated carbon nanotubes were coated onto carbon microfiber electrodes to create a micron-scale bioelectrode. This material has a high surface area and can serve as a support for immobilization of enzymes such as glucose oxidase. A typical carbon nanotube loading of 13 μg cm^{-1} yields a coating thickness of 17 μm and a 2000-fold increase in surface capacitance. The modified electrode was further coated with a biocatalytic hydrogel composed of a conductive redox polymer, glucose oxidase, and a crosslinker to create a glucose bioelectrode. The current density on oxidation of glucose is 16.6 mA cm^{-2} at 0.5 V (vs. Ag/AgCl) in oxygen-free glucose solution. We consider this approach to be useful for designing and characterizing surface treatments for carbon mats and papers by mimicking their local microenvironment.

Keywords Electrocatalysis · Carbon fiber microelectrode · Carbon nanotube · Biofuel cells

Introduction

Biofuel cells generate power from ambient fuels such as plant saps, blood-borne glucose and process byproducts such as glycerol, and are suitable for mobile and distributed power applications [1]. Due to the selectivity of enzymes toward specific reactants and reactions, a conventional fuel cell's membrane and compartments can be eliminated, leading to opportunities for miniaturization [2, 3]. However, achievable current density in biofuel cells is limited by low active-site density and inefficient electron transfer. Current densities of no more than about one mA cm^{-2} have been reported for complete biofuel cells in the literature [4]. This limited achievable current density remains a challenge for the practical application of biofuel cells [5].

High surface area electrodes can increase current density by increasing electrochemically active interfaces within fixed electrode volume. Mesoporous materials are ideal as such host media [6]. Pore sizes of 2 to 50 nm are suitable for biomolecule transport, and large surface area enables increased enzyme utilization. Enzymes have been immobilized in nanoporous silicates [7–13], and polymers such as Nafion® and chitosan [12, 14–16]. These nonconducting materials may be interspersed with carbon aerogels [11, 17, 18], and nanotube matrices [13, 19, 20]. To incorporate enzymes within CNT matrices, direct drop-casting [21], layer-by-layer self-assembly [22] and surface modification of CNTs [23] have been implemented to achieve well-mixed composites.

Multi-scale electrodes, with interconnected macropores that ensure liquid phase fuel transport and micropores that provide large surface area and enhanced catalyst loading, represent the desired electrode morphology. For example carbon paper consists of interlaced 10 μm diameter carbon fibers, with 80% porosity and surface area of 0.17 m^2 cm^{-3}, and has been used to immobilize biocatalysts for oxygen reduction [24] and glucose oxidation reactions [25]. To further increase the surface area and provide nanoporous sub-structure, CNTs have been grown on the carbon paper with chemical vapor deposition, leading to a 100-fold increase in surface area and a 10-fold increase in current density [25]. Ivnitski et al. [26] coated glucose oxidase,

Electronic supplementary material The online version of this article (doi:10.1007/s00604-011-0684-2) contains supplementary material, which is available to authorized users.

H. Wen · V. Nallathambi · D. Chakraborty · S. Calabrese Barton (✉)
Department of Chemical Engineering and Materials Science,
Michigan State University,
East Lansing, MI 48824, USA
e-mail: scb@msu.edu

polyethyleneimine and Nafion on this structure to achieve enhanced direct electron transfer. However, quantitative analysis of such electrodes is complicated by non-homogeneous distribution of surface area and material concentrations in the multi-scale structure; it is therefore desirable to study the micro- and nano-scale process separately.

Carbon fiber microelectrodes (CFME) have also been implemented as electrodes in miniature biofuel cells [2, 4, 27] and provide a platform that mimics the micro-environment of a single fiber of carbon paper. In this capacity, CFMEs have been used to study lithium intercalation in lithium batteries [28]. Various morphologies of biocatalyzed CFMEs have been reported. Pishko et al. used a beveled fiber electrode cross-section to make a glucose sensor [29]. Chen et al. fixed fibers into polycarbonate grooves and cast on the fiber mediator-enzyme adducts that achieved both glucose oxidation and oxygen reduction [27]. F. Gao et al. used the same setup and test condition, but with nanoporous carbon fibers to enhance surface area [23]. Chen et al. used a carbon nanoelectrode modified with CNTs for bio-molecule detection, without any enzyme or mediator coating [30].

In the current work, CFMEs that mimic the morphology and microenvironment of nanotube-coated carbon paper fibers were fabricated and characterized. The CFME has diameter of 7 μm with exposed length of 1 cm. CNT and biocatalyst were coated on the exposed fiber at varied loading to form miniature bio-electrodes. Electrode morphology was characterized scanning electron microscopy (SEM), optical microscopy, and electrochemical capacitance. Bioelectrocatalytic performance was assessed using glucose oxidation catalyzed by mediated glucose oxidase. Understanding of this simple system informs the design and further study of high surface area, multiscale electrodes.

Experimental

Chemicals and materials

Carboxylated multiwall carbon nanotubes (unless mentioned otherwise, CNT hereafter refers to carboxylated CNT) were obtained from Nanocyl (Sambreville, Belgium, http://www.nanocyl.com/). Carbon microfibers of 7 μm diameter were obtained from Goodfellow (Huntingdon, UK, http://www.goodfellow.com/). Conductive carbon paint was purchased from SPI Supplies (West Chester, PA, http://www.2spi.com). Glass capillary was obtained from A-M Systems (Carlsborg, WA, http://www.a-msystems.com/). N,N-dimethylformamide (DMF) was purchased from Fisher BioReagents (Hampton, NH, http://www.fishersci.com). Glucose oxidase (GOx) from *Aspergillus niger* was purchased from Sigma Aldrich (St. Louis, MO, http://www.sigmaaldrich.com). The synthesis of redox polymer Poly(vinylimidazole)-[Os(bipyridine)$_2$Cl]$^{+/2+}$ was reported previously [31]. D-glucose, sodium bicarbonate, sodium phosphate monobasic, sodium phosphate diabasic were purchased from J.T. Baker (Phillipsburg, NJ, http://www.jtbaker.com) and used as received.

CFME fabrication

The schematic of CFME is demonstrated in Fig. 1. Carbon fiber was attached to copper wire with conductive carbon paint, and flame fuse-sealed in the tip of a micropipette by a micropipette puller (Sutter Instrument, Model P-30, Novato, CA, http://www.sutter.com). The exposed fiber was cut to 1 cm with a scalpel.

CNTs were dispersed in DMF to form 1 mg mL^{-1} solution [32]. The DMF/CNT solution was cast to a CFME by brushing a micropipette tip on the electrode fiber. The freshly coated CFME was rinsed with DI water and dried at 70 °C for one hour before use.

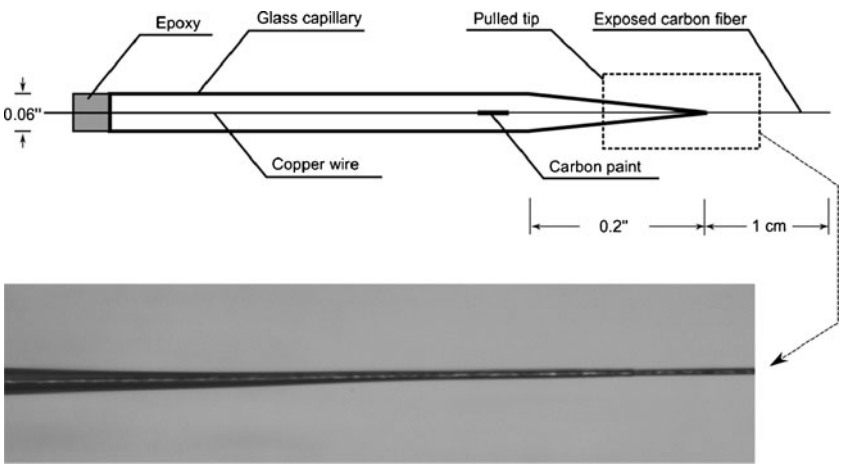

Fig. 1 Carbon fiber microelectrode design. **a**. Electrode diagram with dimensions. **b.** Optical micrograph showing carbon fiber-capillary interface

Surface morphology and surface area characterization

The morphology of the CFME was characterized by both scanning electron microscope (SEM, JEOL JSM-7500F, 5.0 kV accelerating voltage and 2 mm working distance) and optical microscope (Nikon Eclipse LV150, Tokyo, Japan, http://www.nikoninstruments.com). Electrochemical capacitance was measured by cyclic voltammetry at varying scanning rates from 0.4 to 0.5 V vs. Ag/AgCl. Non-faradaic current was plotted against scanning rate, the slope of which was recorded as the capacitance. Surface area was estimated from capacitance using an assumed specific capacitance of 25 μF cm^{-2}, a value that is representative of carbon materials [33].

Biocatalyst coating

Biocatalyst precursor solution was cast onto CFME to form a hydrogel. The preparation of precursor solution was previously reported [24, 25]. A solution of 40 mg mL^{-1} GOx was made with 0.1 M $NaHCO_3$, mixed with 7 mg mL^{-1} sodium periodate at 1:2 volume ratio and cured for one hour in darkness [34, 35]. Finally, 2 μL periodate-oxidized GOx, 8 μL 10 mg mL^{-1} PVI-[Os(bipyridine)$_2$Cl]$^{+/2+}$ redox polymer and 0.5 μL 2.5 mg mL^{-1} PEGDGE were mixed together to yield the precursor solution. Similar to CNT immobilization, a micropipette was used to brush the precursor solution onto CFME, followed by 12-hour curing before further experiments.

Electrochemical characterization

Electrochemical characterization was conducted in a water-jacketed cell containing 50 mL phosphate-buffered saline (PBS, 20 mM phosphate, 0.1 M NaCl, pH 7.0) at 37.5 °C, using a Bio-Logic (Knoxville, TN, http://www.bio-logic.info) VSP potentiostat. Working electrode potential was measured relative to a silver-silver chloride (Ag|AgCl) reference electrode (Fisher Scientific, Hampton, NH), with platinum wire counter electrode. Redox polymer response was characterized by cyclic voltammetry with scan rate at 50 mV/s from 0.0 V to 0.5 V/Ag|AgCl with glucose-free electrolyte and nitrogen sparging to exclude oxygen. Electrode polarization was carried out in the same potential range, but at scan rate of 1 mV s^{-1}, with 50 mM glucose and nitrogen sparging.

Results and discussion

CNT coated CFME

CNT coatings of up to 13 μg cm^{-2} were applied to the carbon fiber surface. Figure 2 shows the scanning electron micrograph of the CFMEs coated with CNTs, indicating significant roughness on the micron scale. On the nano-scale, the nanotubes interlaced into a homogeneous porous material. Pore size was estimated from Fig 2a to be 50 nm on average, suitable for passage of ~10 nm biomolecules. Electrodes with varying CNT loading had the same nano-porous surface but differed in micron-scale roughness and coating thickness, as shown in Fig. 2d-h.

The capacitance and coating thickness of CNT-loaded CFMEs are shown in Fig. 3. As expected, the thickness followed a square root relationship with coating mass. The large standard deviation is due to micron-scale roughness. Capacitance increased 2,000 fold above a bare CFME. Capacitance increases linearly at small CNT loading up to 6 μg, above which the slope decreases, probably due to transport limitations that hinder charge transport to inner NT layers.

Bare CFME coated with hydrogel

As a baseline, bare CFMEs without CNTs were coated with biocatalyst. The coating thickness with varying precursor solution volume is shown in Fig. 4. As expected, the coating thickness is proportional to the square root of applied precursor solution volume. Compared to CNT-

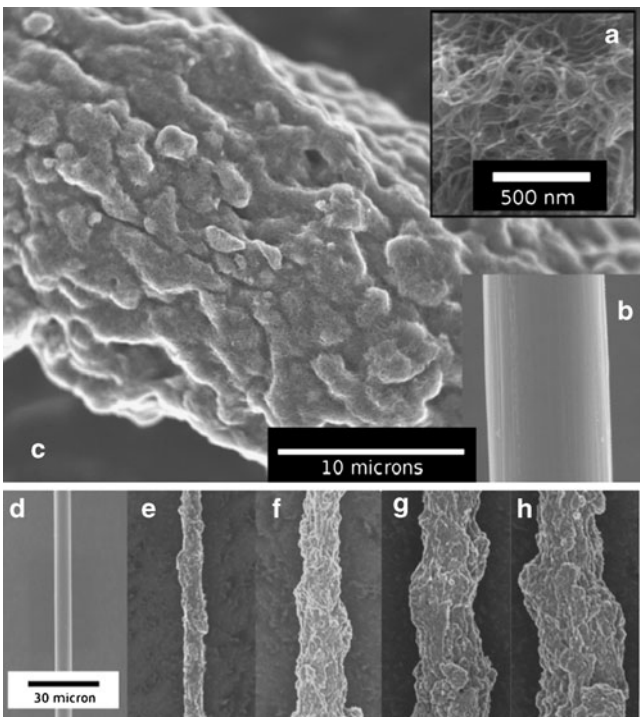

Fig. 2 Scanning electron micrographs of CNT coated CFME. **a**. and **c**. fiber with 2 μg cm^{-1} loading; **b**. Bare carbon fiber control with same scale as (**c**.); **d**-**h**. CFME/CNT morphology with increasing CNT loading: **d**. bare CFME, **e**. 1 μg cm^{-1}, **f**. 2 μg cm^{-1}, **g**., 5 μg cm^{-1}, **h**. 13 μg cm^{-1}

coated CFME surfaces in Fig. 2, the hydrogel coating layer surface is smoother and less varied in thickness (Fig. 4a-f).

The effect of hydrogel film thickness on the current density for glucose oxidation on bare CFMEs is shown in Fig. 5. The inset shows a typical polarization curve for the bioanode. The current density reaches a maximum at 0.3 V/Ag|AgCl, and shows a hysteresis of ~0.2 mA cm^{-2} at 0.3 V. The current densities at 0.5 V for all the film thicknesses are summarized, from which it can be concluded that less than 5 μm of the hydrogel film thickness was active for glucose oxidation, with less than 10% variation in current density from 1 to 15 μm film thickness. At thickness greater than 10 μm, the glucose oxidation current decreased, probably due to transport limitations of glucose and mediator within the hydrogel film.

CFME/CNT/Hydrogel composite electrode

The hydrophilicity of the CNT coating layer directly impacts the loading of hydrogel into the layer, since the hydrogel is highly hydrophilic. For this reason, carboxylated CNT are employed in this work. As demonstrated in Fig. 6, NT-coated CFMEs with hydrogel loading of up to 40 μg cm^{-1} maintain constant layer thickness, suggesting that the hydrogel material has been completely absorbed into the NT layer. Based on the NT loading of 13 μg cm^{-1}, the NT layer can absorb up to 3.1 g of hydrogel per g NTs. Addition of the hydrogel component leads to a more uniform thickness as indicated by the smaller error bars as compared to Fig. 3. Hydrogel coating thickness on bare fibers is also shown and is consistent with the complete absorption of the hydrogel into the NT layer.

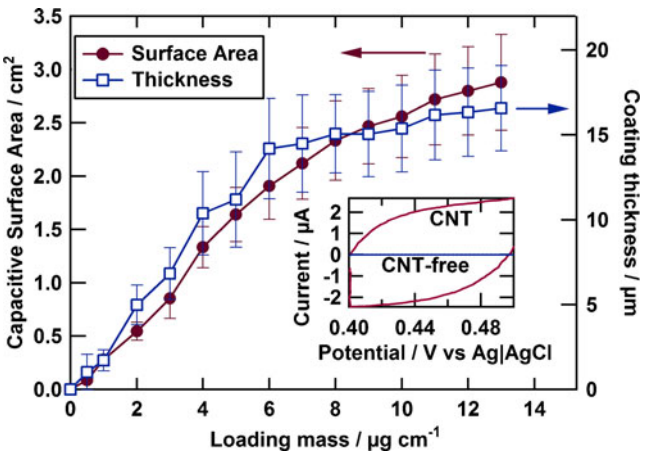

Fig. 3 Surface characterization of CNT-coated CFME. Capacitance obtained by cyclic voltammetry in the 0.4 to 0.5 V/Ag|AgCl range in PBS, pH 7.0, 25 °C. Inset: cyclic voltammetry at 30 mV/s for bare CFME and 13 μg cm^{-1} CNT loaded CFME. Surface area was calculated from capacitance assuming a specific capacitance of 25 μF cm^{-2}

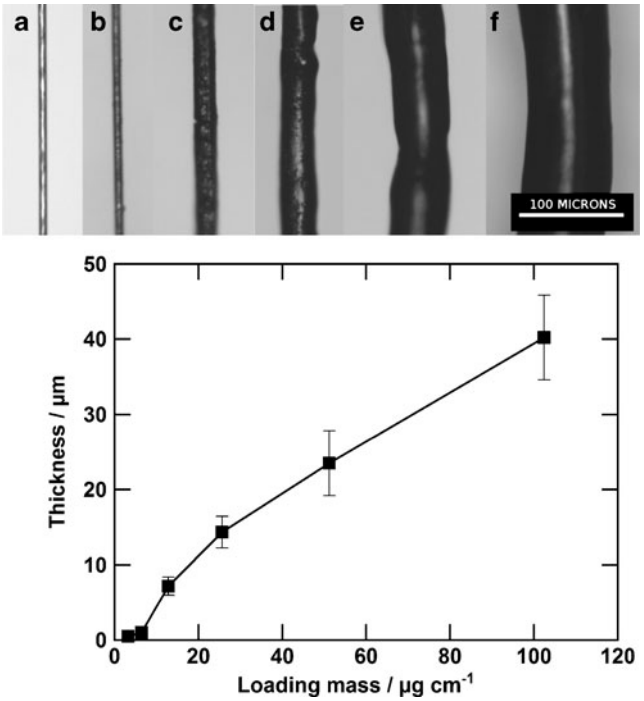

Fig. 4 Biocatalyst-containing hydrogel films cast on a NT-free CFME. *Top*: optical micrographs for precursor solution volume of **a**. 0, **b**. 3.2 μg cm^{-1}, **c**. 12.8 μg cm^{-1}, **d**. 25.6 μg cm^{-1}, **e**. 51.2 μg cm^{-1}, **f**. 102.4 μg cm^{-1}. *Bottom*: summary of the loading and thickness

Electrochemical characterizations of CNT/hydrogel-coated CFMEs are shown in Fig. 7. The top figure shows cyclic voltammograms of three typical samples in the

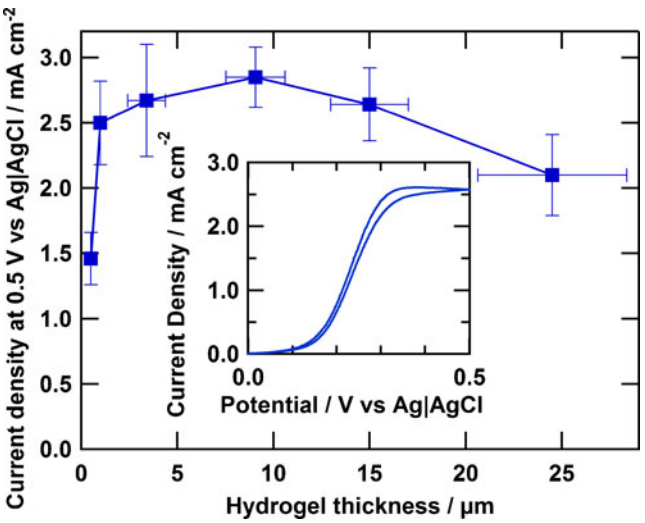

Fig. 5 Effect of hydrogel coating thickness on glucose oxidation rate at NT-free CFME at 0.5 V/Ag|AgCl. Inset: example polarization curve at 15 μm coating thickness. Conditions: nitrogen-purged 50 mM glucose in PBS pH 7, 37.5 °C, scan rate 1 mV s^{-1}, with stirring bar rotating at 150 rpm

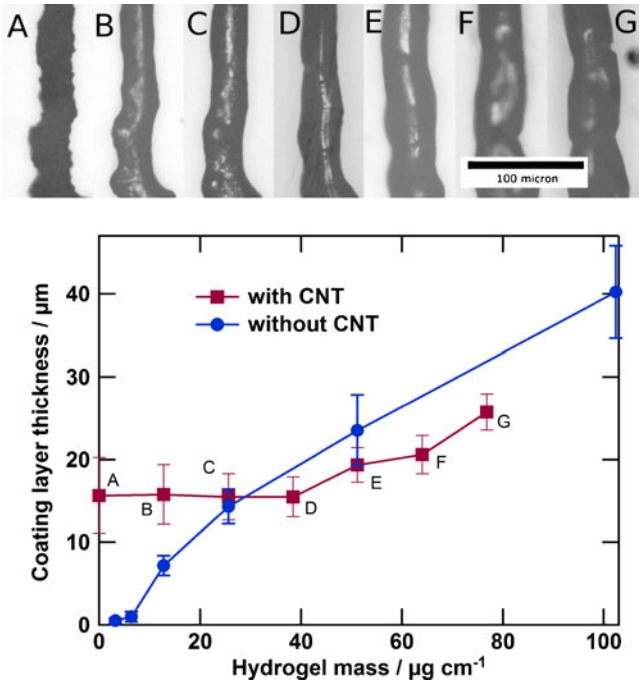

Fig. 6 Hydrogel infiltration into CNT matrix. Hydrogel was coated on 13 µg cm^{-1} CNT-coated CFME at loadings from 0 (**a**) to 76.8 µg cm^{-1} (**g**). Optical micrographs show the change in dry hydrogel coating thickness at the same site. Beyond point D, The pores of the CNT layer were filled, thus the increase of dry thickness beyond point D can be compared to a CNT-free microelectrode

absence of glucose. The observed redox couple is associated with the mediator redox reaction at the electrode. Samples a to c correspond to increasing CNT loadings. For a totally reversible single electron redox reaction, the peak separation should be 56.5 mV at 25 °C [36]. In our system, the peak separation increased from 90 mV for sample a, to 290 mV for sample c. This is an indication of large internal resistance (see Electronic Supplementary Material). The peak height increased from 0.87 to 5.76 mA cm^{-2} due to the increased loading of the redox mediator complex. The mediator activity trend affected the polarization curve (Fig. 7b) in two ways: the current density increased 6.4 fold from 2.58 to 16.63 mA cm^{-2} at 0.5 V, and the mass-transport-controlled plateau current region shifted to the right and was not reached at high mediator loading.

Current density of a larger set of samples at 0.5 V/Ag|AgCl is summarized in Fig. 7-c, where it is shown to correlate linearly with estimated surface area (Fig. 3). Such a linear relationship indicates that the CNT surface area is utilized uniformly by the bioactive materials, even at very high loading (13 µg cm^{-1}) and CNT layer thickness (~17 µm). Diffusional transport of glucose, enhanced by the cylindrical geometry of the electrode, is not substantially hindered by the presence of the nanotubes. Current density is found to vary with glucose concentration according to the expected Michaelis-Menten relationship, with maximum current density and apparent Michaelis constants reported in Electronic Supplementary Material.

Conclusions

A high surface area CNT coated CFME electrode for mediated biocatalysis is shown to provide quantifiable and observable increases in electrode current density. Compared to the bare CFME, the surface area of the modified

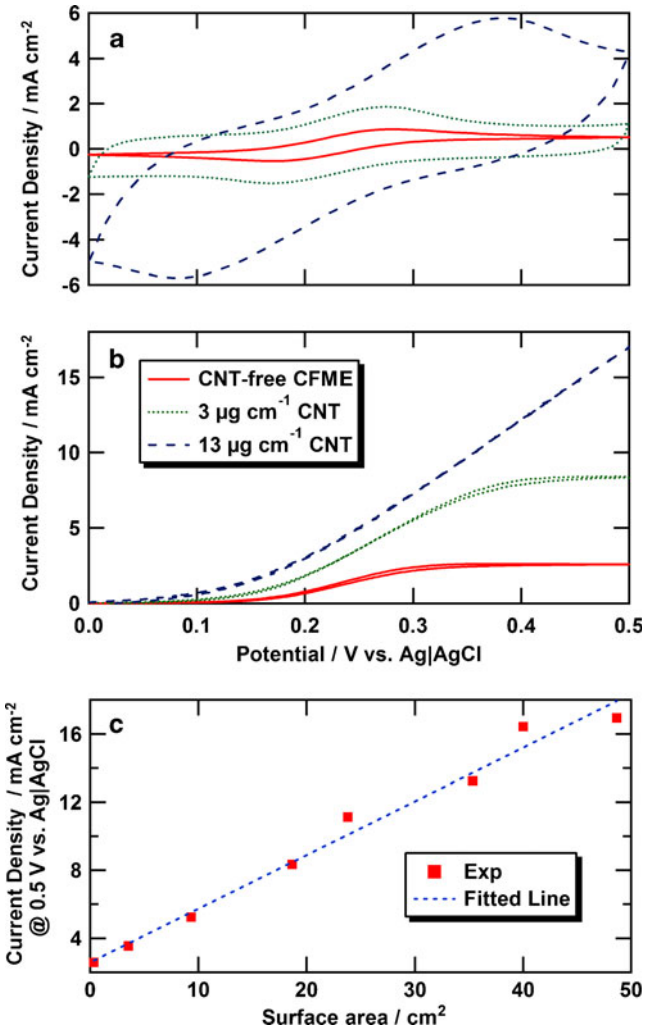

Fig. 7 Electrochemical characterization of CFME/CNT/hydrogel electrodes for three CNT loadings. **a** Redox polymer voltammetry in N_2-purged PBS, pH 7.0, 37.5 °C, glucose-free, at 50 mV/s. **b** Glucose oxidation in the same electrolyte, but with 50 mM glucose at 1 mV/s. Convection was introduced by rotating a magnetic stirring bar at 150 rpm. The samples were all loaded with 26 µg cm^{-1} hydrogel with 39.6 wt% GOx, 59.5 wt% redox polymer and 0.9 wt% PEGDGE. **c** Summary plot of glucose oxidation current density with linear fit

electrode showed more than 2000-fold increase. Thanks to the hydrophilicity of the carboxylated CNT, the biocatalyst precursor solution was absorbed into the porous structure and formed a well-mixed CNT/hydrogel composite. This composite increased the concentration of active mediator and enzyme, and led to a 6.4 fold increase in glucose oxidation current density to 16.63 mA cm^{-2} at 0.5 V/Ag|AgCl. This work lays a foundation for understanding reaction and transport mechanisms in fiber supported bioelectrodes and micro-bioelectrodes for sensors and miniature biofuel cells.

Acknowledgments The authors gratefully acknowledge support from the University of New Mexico under contract FA9550-06-1- 0264 from the Air Force Office of Scientific Research.

References

1. Calabrese Barton S, Gallaway J, Atanassov P (2004) Enzymatic biofuel cells for implantable and microscale devices. Chem Rev 104(10):4867–4886. doi:10.1021/cr020719k
2. Mano N, Mao F, Heller A (2002) A miniature biofuel cell operating in a physiological buffer. J Am Chem Soc 124 (44):12962–12963. doi:10.1021/ja028514g
3. Heller A (2004) Miniature biofuel cells. Phys Chem Chem Phys 6 (2):209–216. doi:10.1039/B313149A
4. Mano N, Mao F, Heller A (2003) Characteristics of a miniature compartment-less glucose–O_2 biofuel cell and its operation in a living plant. J Am Chem Soc 125(21):6588–6594. doi:10.1021/ja0346328
5. Tamaki T, Hiraide A, Asmat FB, Ohashi H, Ito T, Yamaguchi T (2010) Evaluation of immobilized enzyme in a high-surface-area biofuel cell electrode made of redox-polymer-grafted carbon black. Ind Eng Chem Res 49(14):6394–6398. doi:10.1021/ie1001789
6. Kim J, Jia H, Wang P (2006) Challenges in biocatalysis for enzyme-based biofuel cells. Biotechnol Adv 24(3):296–308. doi:10.1016/j.biotechadv.2005.11.006
7. Mano N, Kim H-H, Heller A (2002) On the relationship between the characteristics of bilirubin oxidases and O_2 cathodes based on their "wiring". J Phys Chem B 106(34):8842–8848. doi:10.1021/jp025955d
8. Díaz JF, Balkus KJ (1996) Enzyme immobilization in MCM-41 molecular sieve. J Mol Catal B: Enzym 2(2–3):115–126. doi:10.1016/s1381-1177(96)00017-3
9. Wang P, Dai S, Waezsada SD, Tsao AY, Davison BH (2001) Enzyme stabilization by covalent binding in nanoporous sol-gel glass for nonaqueous biocatalysis. Biotechnol Bioeng 74(3):249–255. doi:10.1002/bit.1114
10. Lei CH, Shin YS, Liu J, Ackerman EJ (2002) Entrapping enzyme in a functionalized nanoporous support. J Am Chem Soc 124 (38):11242–11243
11. Tsionsky M, Gun G, Glezer V, Lev O (1994) Sol-gel-derived ceramic-carbon composite electrodes: introduction and scope of applications. Anal Chem 66(10):1747–1753. doi:10.1021/ac00082a024
12. Qiu J-D, Xie H-Y, Liang R-P (2008) Preparation of porous chitosan/carbon nanotubes film modified electrode for biosensor application. Microchim Acta 162(1):57–64. doi:10.1007/s00604-007-0871-3
13. Ivnitski D, Artyushkova K, Rincón R, Atanassov P, Luckarift H, Johnson G (2008) Entrapment of enzymes and carbon nanotubes in biologically synthesized silica: glucose oxidase-catalyzed direct electron transfer. Small 4(3):357–364. doi:10.1002/smll.200700725
14. Liu Y, Wang M, Zhao F, Xu Z, Dong S (2005) The direct electron transfer of glucose oxidase and glucose biosensor based on carbon nanotubes/chitosan matrix. Biosens Bioelectron 21(6):984–988. doi:10.1016/j.bios.2005.03.003
15. Klotzbach T, Watt M, Ansari Y, Minteer SD (2006) Effects of hydrophobic modification of chitosan and Nafion on transport properties, ion-exchange capacities, and enzyme immobilization. J Membr Sci 282(1–2):276–283. doi:10.1016/j.memsci.2006.05.029
16. Cooney MJ, Lau C, Windmeisser M, Liaw BY, Klotzbach T, Minteer SD (2008) Design of chitosan gel pore structure: towards enzyme catalyzed flow-through electrodes. J Mater Chem 18 (6):667–674. doi:10.1039/B710082e
17. Morris CA, Anderson ML, Stroud RM, Merzbacher CI, Rolison DR (1999) Silica sol as a nanoglue: flexible synthesis of composite aerogels. Science 284(5414):622–624. doi:10.1126/science.284.5414.622
18. Yang C-M, Choi W-H, Na B-K, Cho BW, Cho WI (2005) Capacitive deionization of NaCl solution with carbon aerogel-silicagel composite electrodes. Desalination 174(2):125–133. doi:10.1016/j.desal.2004.09.006
19. Wang J, Gu M, Di J, Gao Y, Wu Y, Tu Y (2007) A carbon nanotube/silica sol–gel architecture for immobilization of horseradish peroxidase for electrochemical biosensor. Bioproc Biosyst Eng 30(4):289–296. doi:10.1007/s00449-007-0126-z
20. Gavalas VG, Law SA, Christopher Ball J, Andrews R, Bachas LG (2004) Carbon nanotube aqueous sol-gel composites: enzyme-friendly platforms for the development of stable biosensors. Anal Biochem 329(2):247–252. doi:10.1016/j.ab.2004.02.025
21. Wang J, Li M, Shi Z, Li N, Gu Z (2002) Direct electrochemistry of cytochrome c at a glassy carbon electrode modified with single-wall carbon nanotubes. Anal Chem 74(9):1993–1997. doi:10.1021/ac010978u
22. Deng L, Shang L, Wang Y, Wang T, Chen H, Dong S (2008) Multilayer structured carbon nanotubes/poly-l-lysine/laccase composite cathode for glucose/O_2 biofuel cell. Electrochem Commun 10(7):1012–1015. doi:10.1016/j.elecom.2008.05.001
23. Gao F, Viry L, Maugey M, Poulin P, Mano N (2010) Engineering hybrid nanotube wires for high-power biofuel cells. Nat Commun 1(1):1–7. doi:10.1038/ncomms1000
24. Barton S, Kim H-H, Binyamin G, Zhang Y, Heller A (2001) Electroreduction of O_2 to water on the "wired" Laccase Cathode. J Phys Chem B 105(47):11917–11921. doi:10.1021/jp012488b
25. Barton S, Sun Y, Chandra B, White S, Hone J (2007) Mediated enzyme electrodes with combined micro- and nanoscale supports. Electrochem Solid State Lett 10(5):B96–B100. doi:10.1149/1.2712049
26. Ivnitski D, Branch B, Atanassov P, Apblett C (2006) Glucose oxidase anode for biofuel cell based on direct electron transfer. Electrochem Commun 8(8):1204–1210. doi:10.1016/j.elecom.2006.05.024
27. Chen T, Barton SC, Binyamin G, Gao ZQ, Zhang YC, Kim HH, Heller A (2001) A miniature biofuel cell. J Am Chem Soc 123 (35):8630–8631. doi:10.1021/ja0163164
28. Verbrugge MW, Koch BJ (1996) Modeling lithium intercalation of single-fiber carbon microelectrodes. J Electrochem Soc 143 (2):600–608. doi:10.1149/1.1836486
29. Pishko M, Michael A, Heller A (1991) Amperometric glucose microelectrodes prepared through immobilization of glucose oxidase in redox hydrogels. Anal Chem 63(20):2268–2272. doi:10.1021/ac00020a014
30. Chen R-S, Huang W-H, Tong H, Wang Z-L, Cheng J-K (2003) Carbon fiber nanoelectrodes modified by single-walled carbon nanotubes. Anal Chem 75(22):6341–6345. doi:10.1021/ac0340556

31. Gregg B, Heller A (1991) Redox polymer films containing enzymes. 1. A redox-conducting epoxy cement: synthesis, characterization, and electrocatalytic oxidation of hydroquinone. J Phys Chem 95(15):5970–5975. doi:10.1021/j100168a046
32. Freiman S, Hooker S, Migler K, Arepalli S (2008) Measurement issues in single wall carbon nanotubes. National Institute of Standards and Technology, Gaithersburg
33. Kinoshita K (1988) Carbon: electrochemical and physicochemical properties. Wiley, New York
34. Binyamin G, Heller A (1999) Stabilization of wired glucose oxidase anodes rotating at 1000 rpm at 37 °C. J Electrochem Soc 146(8):2965–2967. doi:10.1149/1.1392036
35. Zaborsky O (1974) The immobilization of glucose oxidase via activation of its carbohydrate residues. Biochem Biophys Res Commun 61(1):210–216. doi:10.1016/0006-291X(74)90554-3
36. Bard AJ, Faulkner LR (2004) Electrochemical methods fundamentals and applications, 2nd edn. Wiley, New York